Phase Noise Effects on Square-QAM Symbol Error Rate Performance

James A. Crawford

Phase noise is an increasingly serious performance issue as the order of the QAM signal constellation is increased. This brief memo derives a formula to compute the QAM symbol error rate when phase noise is present with coherent demodulation. Only square QAM signal constellations will be considered.

Let M^2 be the total number of points used in the signal constellation. This is equivalent to using M signal levels on the I and Q rails each. Further assume that the (voltage) distance between signal levels on the I and Q rails is d. A 16-QAM signal constellation is shown here for example in Figure 1.

Figure 1 Sample QAM Signal Constellation for 16-QAM Case

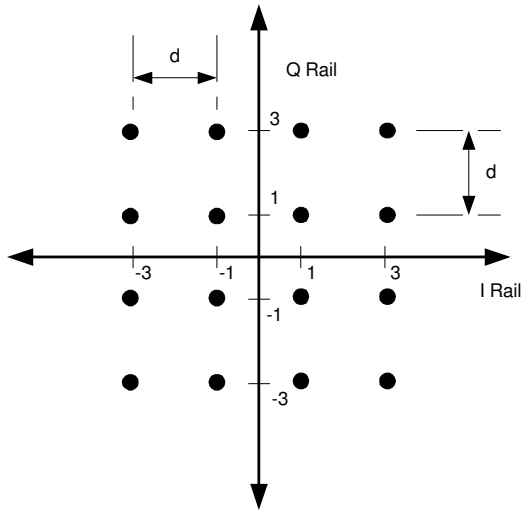

Figure 2 Average Energy per Symbol for Square QAM Constellations

M^2	M	Ave. Energy per Symbol/d^2
4	2	2/4
16	4	10/4
64	8	42/4
256	16	170/4
1024	32	682/4

Assume that a data-symbol represented by the coordinate pair (a_k, b_k) is transmitted. After reception by a receiver, the baseband I,Q signals are given by

$$\begin{aligned} I_k &= \text{Real}\left[\left(a_k + jb_k\right)e^{j\varphi_n}\right] \\ &= a_k\cos(\varphi_n) - b_k\sin(\varphi_n) + n_I \\ Q_k &= \text{Imag}\left[\left(a_k + jb_k\right)e^{j\varphi_n}\right] \\ &= a_k\sin(\varphi_n) + b_k\cos(\varphi_n) + n_I \end{aligned} \quad (1)$$

where φ_n represents a phase term due to the recovered phase error and or local oscillator phase noise, and n_I and n_Q are additive Gaussian noise terms each having variance σ^2. This can be conveniently re-written in matrix form as

$$\begin{bmatrix} I_k \\ Q_k \end{bmatrix} = \begin{bmatrix} \cos(\varphi_n) & -\sin(\varphi_n) \\ \sin(\varphi_n) & \cos(\varphi_n) \end{bmatrix}\begin{bmatrix} a_k \\ b_k \end{bmatrix} + \begin{bmatrix} n_I \\ n_Q \end{bmatrix} \quad (2)$$

The I and Q channels are cross-coupled due to the common phase noise term φ_n. The cross-talk between the I and Q channels is severe because it is weighted by the first-order $\sin(\varphi_n)$ term, and also weighted by the potentially much stronger signal amplitude in the other channel.

Decision thresholds on the I and Q rails are the same when the signal level is properly normalized by automatic gain control (AGC). These detection thresholds are shown in Figure 3.

Figure 3 16-QAM I and Q Rails with Detection Regions

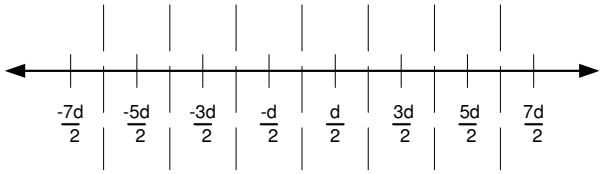

Except for the endpoints on each rail, a symbol error occurs if the noise plus interference is greater than d/2.

I Signal Rail

A decision error on either I- or Q-channel results in a symbol error. The I- and Q-channels can be handled independently and the results combined. Attention is focused on the I-channel here.

For all of the interior points on the I-rail (i.e., less endpoints), a symbol error occurs if

$$\left|a_k \cos(\varphi_n) - b_k \sin(\varphi_n) + n_I - a_k\right| > \frac{d}{2} \quad (3)$$

NOTE: For practical QAM usage, the phase noise will be reasonably small in which case $|\varphi_n|$ will be kept reasonably small also. Take for example cos(5°)= 0.9962 whereas sin(5°)= 0.0872. In general, we can ignore the cos²( ) coherence loss term in steady-state operation because $|\varphi_n| \ll \pi/4$

With this simplifying assumption, a symbol error occurs due to a decision error on the I-rail if

$$\left|b_k \sin(\varphi_n) - n_I\right| > \frac{d}{2} \quad (4)$$

Since n_I is mean-zero and Gaussian distributed, we know that

$$p(n_I) = \frac{1}{\sqrt{2\pi}\sigma} \exp\left[-\frac{n_I^2}{2\sigma^2}\right] \quad (5)$$

Let the observed interference plus noise be represented by

$$v = b_k \sin(\varphi_n) - n_I \quad (6)$$

then

$$p(v) = \frac{1}{\sqrt{2\pi}\sigma} \exp\left[-\frac{\left[v - b_k \sin(\varphi_n)\right]^2}{2\sigma^2}\right] \quad (7)$$

The probability of error on the I-rail for each of the interior constellation points is then given by

$$P_{error}(b_k, \varphi_n) = 2\int_{d/2}^{\infty} \frac{1}{\sqrt{2\pi}\sigma} \exp\left[-\frac{\left[v - b_k \sin(\varphi_n)\right]^2}{2\sigma^2}\right] dv \quad (8)$$

Letting $u = v - b_k \sin(\varphi_n)$ and substituting,

$$P_{error}(b_k, \varphi_n) = erfc\left[\frac{\frac{d}{2} - b_k \sin(\varphi_n)}{\sqrt{2}\sigma}\right] \quad (9)$$

For the endpoints, when $\left|b_k \sin(\varphi_n) - n_I\right| > \frac{d}{2}$, a symbol error only occurs one-half of the time. Therefore, for the average I-channel probability that the wrong sample value is decided on is given by

$$P_{SI}(b_k, \varphi_n) = \frac{(M-1)}{M} erfc\left[\frac{\frac{d}{2} - b_k \sin(\varphi_n)}{\sigma\sqrt{2}}\right] \quad (10)$$

Similarly for the Q-channel,

$$P_{SQ}(a_k, \varphi_n) = \frac{(M-1)}{M} erfc\left[\frac{\frac{d}{2} - a_k \sin(\varphi_n)}{\sigma\sqrt{2}}\right] \quad (11)$$

The probability that any given symbol is received without error is then $P_c = (1-P_{SI})(1-P_{SQ}) \approx 1 - P_{SI} - P_{SQ}$. Due to the symmetric results for the I- and Q-channels along with the statistical independence assumed between the data symbol ingredients a_k and b_k, this leads finally to

$$P_{sym}(\varphi_n) = 2\left(\frac{M-1}{M}\right)\left\langle erfc\left[\frac{\frac{d}{2} - a_k \sin(\varphi_n)}{\sigma\sqrt{2}}\right]\right\rangle \quad (12)$$

where the angular brackets denote averaging over the a_k's.

For M points on each I and Q rail,

$$a_k = \frac{2k+1}{2} d \quad (13)$$

for k=0…(M/2)-1 for one-half of the levels, and the negative of these values for the other half. Therefore,

$$P_{sym}(\varphi_n) = 2\left(\frac{M-1}{M^2}\right)\bullet \sum_{k=0}^{\frac{M}{2}-1}\left\{ erfc\left[\frac{\frac{d}{2}-\frac{2k+1}{2}d\sin(\varphi_n)}{\sigma\sqrt{2}}\right] + erfc\left[\frac{\frac{d}{2}+\frac{2k+1}{2}d\sin(\varphi_n)}{\sigma\sqrt{2}}\right]\right\} \quad (14)$$

In order to calculate σ^2 in the present context in terms of SNR, we can compute the average energy per symbol as

$$E_s = \frac{4}{M^2}\sum_{k=0}^{\frac{M}{2}-1}\sum_{p=0}^{\frac{M}{2}-1}\left[a_k^2 + b_p^2\right] \quad (15)$$

The average energy per bit is then

$$E_b = \frac{E_s}{2\log_2(M)} = \frac{E_s}{\log_2(M^2)} \quad (16)$$

This leads finally to

$$\sigma^2 = \frac{E_s}{2\left(\frac{C}{N}\right)} \quad (17)$$

For the last step, in order to compute the final symbol error rate under normal operating conditions, we assume that φ_n has a Tikhonov distribution. This function formally has a Bessel function involved, but if the probability density function is evaluated for large values of φ_n, some numerical problems can arise. An almost equivalent form that is better behaved numerically is given by

$$p_{\theta_n}(\varphi_n) = \frac{1}{\sigma_{\varphi_n}\sqrt{2}}\exp\left[\frac{\cos(\varphi_n)-1}{\sigma_{\varphi_n}{}^2}\right] \quad (18)$$

where σ_{φ_n} is the integrated phase noise in units of radians rms. The symbol error rate with the phase noise included is at last given by

$$P_{SymErr} = \int_{-\infty}^{+\infty} P_{Sym}(\varphi_n)\, p_{\theta_n}(\varphi_n)\, d\varphi_n \quad (19)$$

Sample Results

Sample results for 16-QAM and 64-QAM are shown here in Figure 4 and Figure 5 respectively. Not surprisingly, the sensitivity of 64-QAM to phase noise is very high. The residual error floor is very apparent and there is clear motivation for trying to design the system such that it operates with an (uncoded) SER more in the range of 10^{-3} where the phase noise impact is less than say at 10^{-5}.

NOTE: The symbol error rate with no phase noise is given by[1]

$$P_{sym}(\gamma_b, M, k) = 2\left(\frac{M-1}{M}\right) erfc\left[\sqrt{\frac{3k\gamma_b}{2\left(M^2-1\right)}}\right]\bullet \left[1-\frac{1}{2}\left(\frac{M-1}{M}\right) erfc\left[\sqrt{\frac{3k\gamma_b}{2\left(M^2-1\right)}}\right]\right] \quad (20)$$

where γ_b is the SNR per bit, k is the number of bits per symbol, and M is the number of levels on each rail. For the 16-QAM case at hand, M=4 and k=4.

[1] Proakis, *Digital Communications*, 2nd Edition, 1989 page 282, equ. (4.2.144)

Figure 4 SER with Phase Noise for 16-QAM

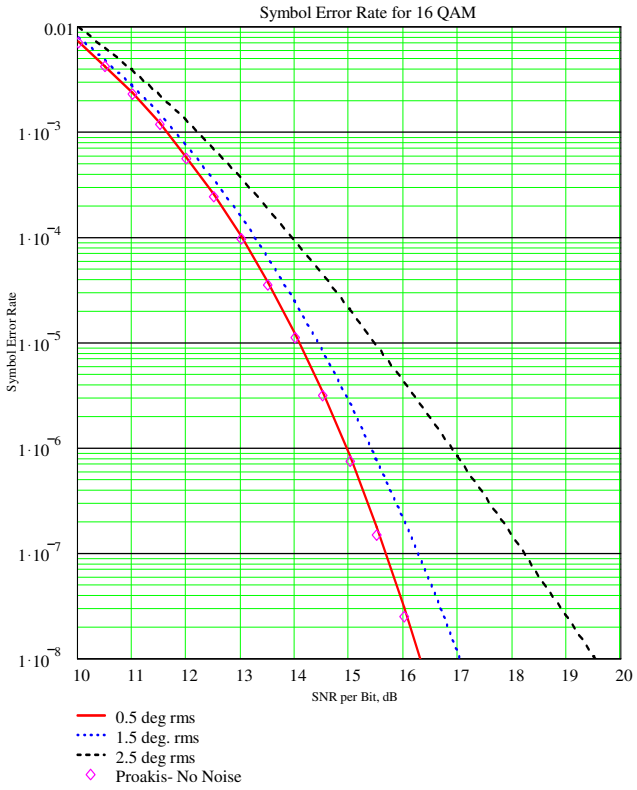

Figure 5 SER for 64-QAM with Phase Noise

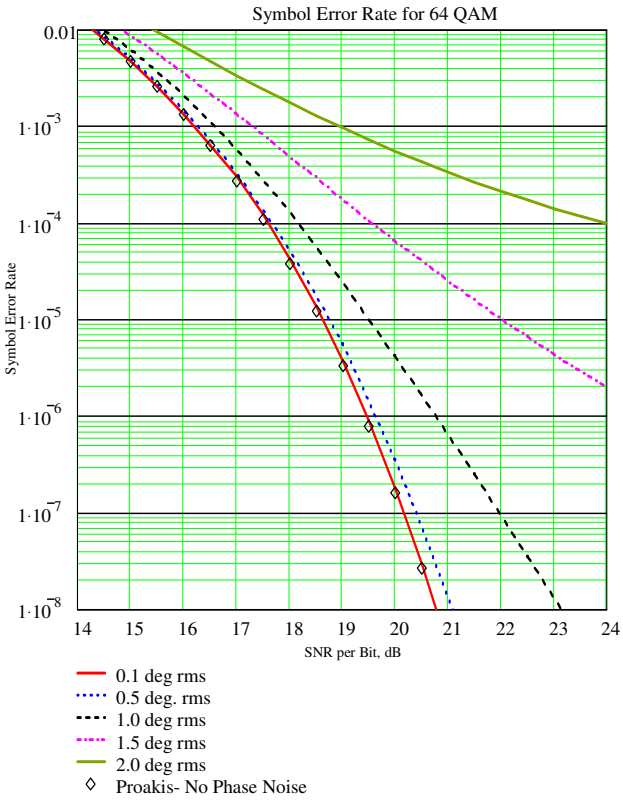

References

1. John G. Proakis, *Digital Communications*, 2nd Edition, McGraw-Hill Book, 1989
2. Marvin K. Simon, et al., *Digital Communication Techniques*, Prentice-Hall, 1995
3. James A. Crawford, *Frequency Synthesizer Design Handbook*, Artech House, 1994

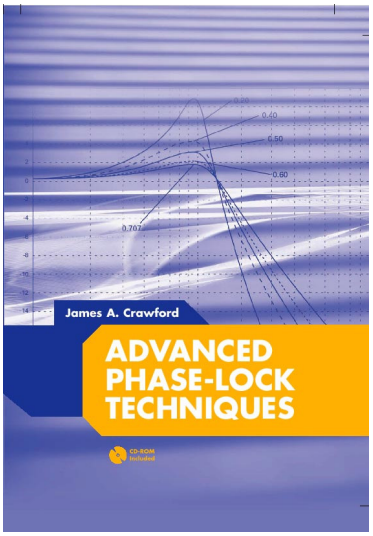

Advanced Phase-Lock Techniques

James A. Crawford

2008

Artech House

510 pages, 480 figures, 1200 equations
CD-ROM with all MATLAB scripts

ISBN-13: 978-1-59693-140-4
ISBN-10: 1-59693-140-X

Chapter	Brief Description	*Pages*
1	*Phase-Locked Systems—A High-Level Perspective* An expansive, multi-disciplined view of the PLL, its history, and its wide application.	26
2	*Design Notes* A compilation of design notes and formulas that are developed in details separately in the text. Includes an exhaustive list of closed-form results for the classic type-2 PLL, many of which have not been published before.	44
3	*Fundamental Limits* A detailed discussion of the many fundamental limits that PLL designers may have to be attentive to or else never achieve their lofty performance objectives, e.g., Paley-Wiener Criterion, Poisson Sum, Time-Bandwidth Product.	38
4	*Noise in PLL-Based Systems* An extensive look at noise, its sources, and its modeling in PLL systems. Includes special attention to 1/*f* noise, and the creation of custom noise sources that exhibit specific power spectral densities.	66
5	*System Performance* A detailed look at phase noise and clock-jitter, and their effects on system performance. Attention given to transmitters, receivers, and specific signaling waveforms like OFDM, M-QAM, M-PSK. Relationships between EVM and image suppression are presented for the first time. The effect of phase noise on channel capacity and channel cutoff rate are also developed.	48
6	*Fundamental Concepts for Continuous-Time Systems* A thorough examination of the classical continuous-time PLL up through 4^{th}-order. The powerful Haggai constant phase-margin architecture is presented along with the type-3 PLL. Pseudo-continuous PLL systems (the most common PLL type in use today) are examined rigorously. Transient response calculation methods, 9 in total, are discussed in detail.	71
7	*Fundamental Concepts for Sampled-Data Control Systems* A thorough discussion of sampling effects in continuous-time systems is developed in terms of the *z*-transform, and closed-form results given through 4^{th}-order.	32
8	*Fractional-N Frequency Synthesizers* A historic look at the fractional-N frequency synthesis method based on the U.S. patent record is first presented, followed by a thorough treatment of the concept based on Δ-Σ methods.	54
9	*Oscillators* An exhaustive look at oscillator fundamentals, configurations, and their use in PLL systems.	62
10	*Clock and Data Recovery* Bit synchronization and clock recovery are developed in rigorous terms and compared to the theoretical performance attainable as dictated by the Cramer-Rao bound.	52